Transactions of the Korean Nuclear Society Spring Meeting
Jeju, Korea, May 7-8, 2015

CFD investigation the thermal-hydraulic behavior behind the flow blockage in SFR

Jin Yoo*, J. H. Jeong, W. P Chang, K. S Ha
Korea Atomic Energy Research Institute
P.O.Box 105, Yuseong, Daejeon, 305-600, Korea
Corresponding author: yoojin@kaeri.re.kr

1. Introduction

The partial flow blockage in a subassembly of an SFR is of importance to the plant safety because of the compact design and high power density of the core. When a partial blockage occurs, sodium coolant flow will be disturbed in the vicinity of the blockage, which may eventually lead to a rupture of the cladding. It is evident that the flow blockage is basically a local phenomenon, and the main issue to investigate is the thermal-hydraulic behavior of the region downstream from the obstacle because it determines the clad temperature peak. For this reason, a local detailed CFD analysis has been carried out in order to assess the impacts of a flow blockage.

The flow blockage events are classified into two types, internal and external blockage, depending on their locations. External flow blockage occurs at the core outlet due to the complex geometry of internal structures above the core outlet. Internal flow blockage occurs at the core inlet due to the presence of foreign material in the primary coolant, a wire wrap failure, excessive pin bowing, and excessive clad swelling

In this regard, internal and planar blockages were considered to cover the adjoining sub-channels in the same axial location, i.e., a six-sub-channel blockage surrounding a pin, such as in ORNL experiments

The objective of this paper is to investigate the influence caused by a flow blockage.

2. Computational conditions

2.1 General Considerations

The computational domain includes an active region with a 900 mm length. The thermal-physical properties applied to the temperature variations are considered to be a fluid composed of Sodium (Na), a solid composed of a clad (HT9), and the blockage material (HT9), as shown in Tables 1 and 2.

Table 1. Physical properties of sodium at 390 ℃

Parameters	Unit	Value at the inlet
Density	Kg/m3	864.1
Dynamic viscosity	Pa s	0.0002808
Thermal Conductivity	W/m K	70.02
Specific heat	J/kg K	1286
Pr	-	0.005156
Re	-	5×10^4

Table 2. Physical properties of HT9 at 390 ℃

Parameters	Unit	Value at the inlet
Density	Kg/m3	7720
Thermal Conductivity	W/m K	25
Specific heat	J/kg K	503

2.2 PGSFR fuel assembly

The main design parameters used in the calculation are listed in Table 3. Figure 1 shows a lateral view sketch of the PGSFR fuel assembly. The fuel assembly of the PGSFR has 217-pin rods helically wire-wrapped, with rod diameter d = 7.4mm, pitch to diameter ratio p/d = 1.203 and active length L = 900mm. The total thermal power of the fuel assembly is Q = 5.1–4.2MW. However, the fuel assembly with a 91-pin rod shown in Figure 2 was considered to restrict the limitations of the required computer memory in this study.

Table 3. Design parameters of the fuel assembly

Parameters	Unit	
Number of Pins	EA	217
Diameter of Pins	mm	7.4
Pin Pitch	mm	8.9
Pitch to diameter	-	1.203
Active core length	mm	900
Wire wrap Pitch	mm	183.8
Diameter of Spacer Wire	mm	1.4
Inner Flat-to-flat Distance	mm	90.604
Power	MW	5.1~4.2
Mass flow rate	Kg/s	11.41

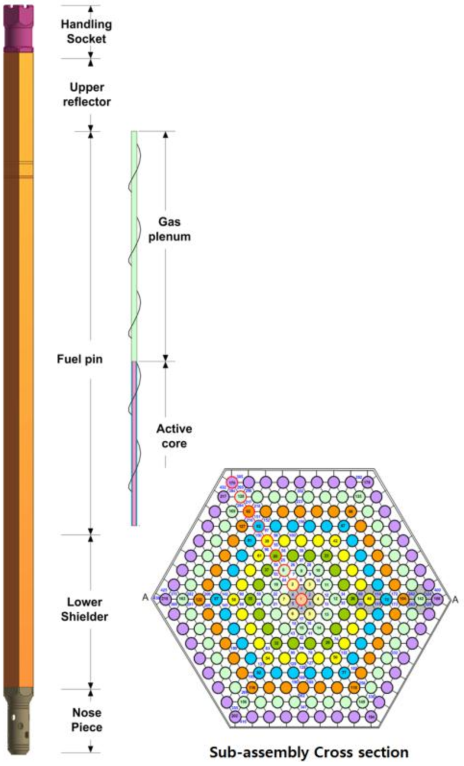

Figure 1. Fuel assembly with 217-pin rods

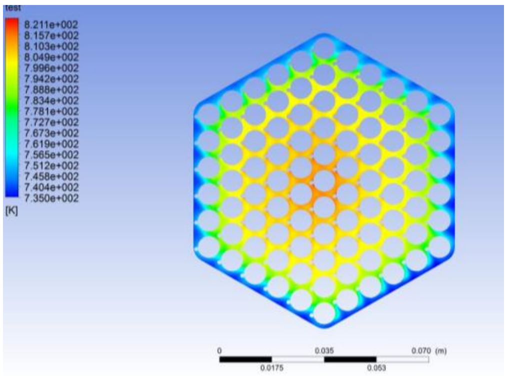

Figure 2. Fuel assembly with 91-pin rods

2.3 Turbulent model and CFD analysis methods

The flow and heat transfer in the rod bundle are governed by the conservation equations of mass, momentum, and energy in the coolant fluid. The coolant flow encountered in wire wrap rod bundles of a fuel assembly is highly turbulent. The presence of a wire wrap surrounding each rod causes both large and small-scale turbulent mixing in a coolant flow. For an accurate representation of turbulence, a direct numerical simulation using a fine grid and transient marching with small time steps is required for resolving all relevant turbulent flows. Such studies are computationally intensive, demanding large computer resources. Therefore, a practical approach involves the accounting of the thermal hydraulic effects of turbulence on the momentum and heat transport simulated through approximate models.

The turbulence modeling is commonly conducted using the Reynolds-averaged Navier-Stokes (RANS) equations. The Reynolds stresses appearing in these equations can be algebraically evaluated with the help of the turbulent eddy viscosity concept. The eddy viscosity, in turn, can be obtained using approaches of different levels of complexity (Launder and Spalding, 1974). It is possible to solve for the Reynolds stresses using six transport equations, with additional computational effort. The turbulence models such as the k-epsilon and k-omega have become industry standard models and are commonly used for most types of engineering problems. The k-omega model is used in the inner parts of the boundary layer, whereas the k-epsilon model is used in the free stream because the prior model is too sensitive to the inlet free-stream turbulence properties. In addition, the SST model combines the effects of the k-omega model, which uses the specific dissipation, omega, and k-epsilon model. The SST model performs well for cases of adverse pressure gradients and a separated flow. This structural feature of the model to predict in a good way the flow separation and recirculation provides a high level of confidence in applying the model to compute the flow blockage in a fuel assembly. Therefore, the SST model was used for the numerical simulations presented in the paper. The high-resolution scheme was used for the convective term. Convergence of the simulation was judged by the periodic temperature on the outlet domain of the 91-pin fuel assembly.

2.4 Computational Boundary Conditions

The boundary conditions imposed on this study are presented in Figure 3. The inlet condition was imposed on a mass flow rate of 11.41 kg/s and constant temperature of 663.15 K, which are equivalent to the assembly conditions with a 217 fuel pin. In addition, the outlet condition was imposed on the relative pressure of 0 Pa. Figure 4 shows the axial heat flux of the fuel assembly in the PGSFR. Heat flux distributions were imposed on the inner cladding surface. In addition, for the outer cladding, the wire was defined with no slip conditions, a conservative interface flux, and a smooth surface. The hexagonal wall of the fluid is taken to be adiabatic. The flow blockage was assumed to take place near the axial position with the highest heat flux in Figure 4. The assumption was based on the background that the coolant heat-up would be large at that position because the flow would slow down or may be temporarily stagnant in the vicinity of the blockage. Figure 5 shows the representative sub-channels for the analysis chosen for the analysis results.

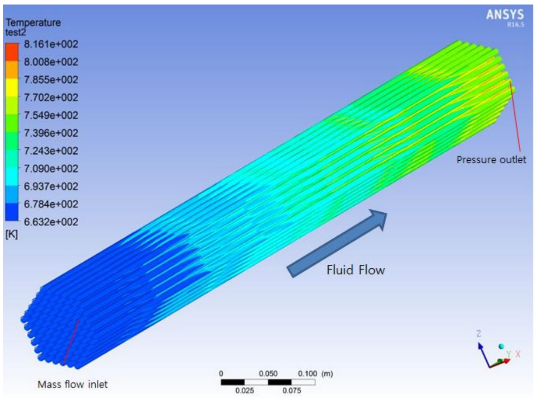

Figure 3. Boundary conditions

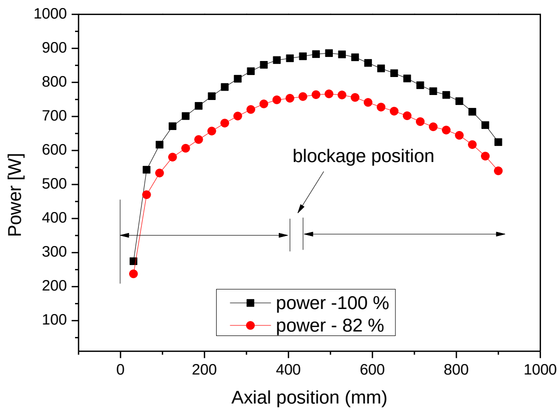

Figure 4. Fuel assembly with 217-pin rods

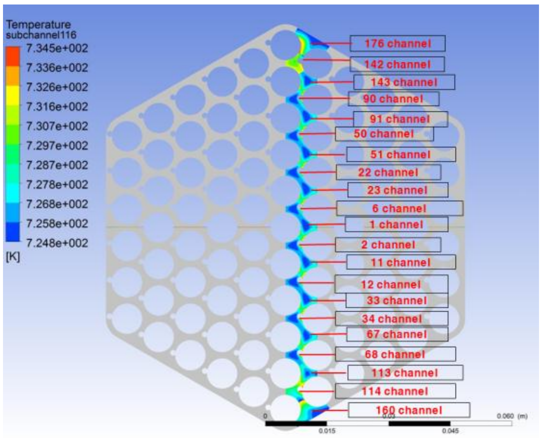

Figure 5. Predicted sub-channel number

3. Results

3. 1 Without blockage

The solution without a blockage is analyzed as a reference to check if the model provides reasonable results and to have a baseline to evaluate the effect of the blockage. Figure 6 shows the vertical velocity contours in a longitudinal transversal plane ZX of the computational domain. It shows that the velocity around the wall of the fluid shows peak values due to the fact that the position of the wire wrap changes from one pitch to another. Figure 7 shows the velocity distribution of the fluid at 440mm, 470mm and 900mm positions from the start of the inlet. The velocity distribution shows an evenly balanced tendency in the central region behind the 470mm position from the inlet. This means that the flow in a hexagonal duct is fully developed within 500 mm. This is because the presence of a wire wrap reduces the axial flow area of the subchannel. Figure 8 shows the temperature contours in a longitudinal plane ZX. It shows that the coolant temperature gradually increases as it flows upward along the end of the active region, and the maximum coolant temperature is estimated at the end of the active core. Figure 9 shows the temperature distribution of the fluid at 440mm, 470mm, and 900mm positions from the start of the inlet. Considering the uniform temperature distribution in the central region, the existence of a wire wrap causes more coolant mixing inside the sub-channel, and hence the temperature distribution has a tendency to be flat in the central region. On the other hand, the sub-channel temperature in the peripheral region, which has less effect on the wire wrap, is lower than in the central region. The coolant temperature reaches up to 530℃ at the end of the active region.

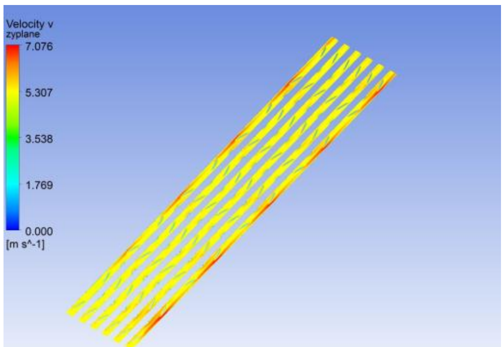

Figure 6 Streamwise velocity contours in the symmetry ZX plane.

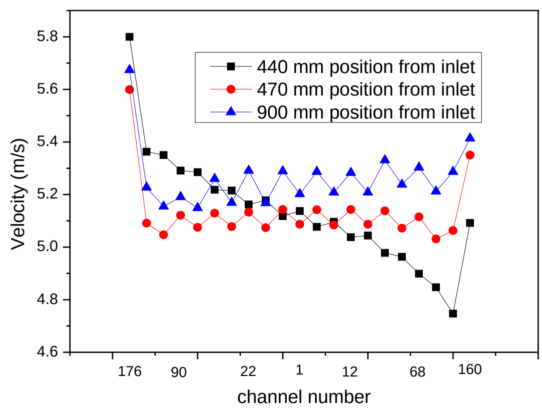

Figure 7 Velocity distributions in the symmetry ZX planes from the start of the inlet

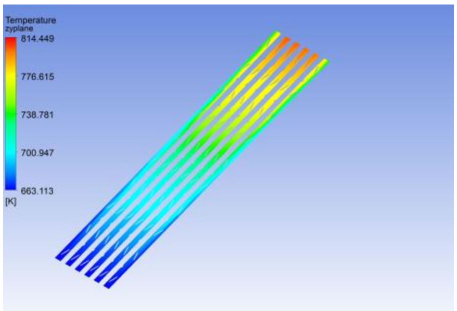

Figure 8 Temperature contours in the symmetry ZX plane

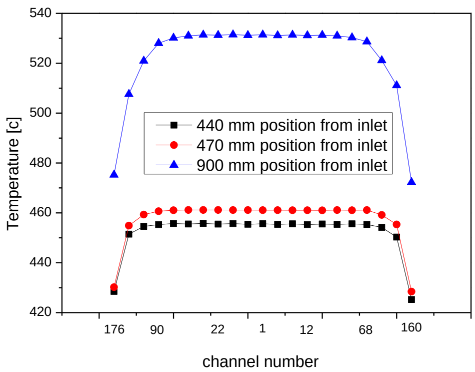

Figure 9 Temperature distributions in the symmetry ZX planes from the start of the inlet

3.2 With blockage

A 3D view of the computational domain modeled with blockage. The blockage is located in the middle of the active region, as shown in Figure 10, where the heat flux is maximum. For cases with a flow blockage, the nominal power condition in a fuel assembly, which is 5.1 MW, has been imposed on the CFD computations.

Figure 11 shows the streamwise velocity contours in the ZX mid-plane. As shown in Figure 11, there is a reduced velocity around the blockage region and the velocity far upstream of the blockage remains unperturbed. Figures 12 and 13 show the velocity contours and distribution downstream from the blockage. From a hydrodynamic point of view, the perturbation on the flow caused by the blockage is local with a small recirculation region downstream from the blockage. In addition, the reduced velocity is dominant within a 470 mm distance from the blockage region. It shows that the recirculation region is certainly less than at a 100 mm distance from the blockage region considering that the streamwise velocity is stabilized at a 500 mm position downstream from the blockage. Figure 14 shows temperature contours in the ZX. The maximum cladding temperature downstream from the blockage is located in the central pins of the blocked region and its temperature is about 1000 ℃. It is closely related to the obstruction of convective heat transfer by the long axial length of the blockage, i.e., 31 mm. Figures 15 and 16 show the temperature contours downstream from the blockage. It shows that the effect of temperature increase is dorminant from the start of the blockage to the end of the 470 mm axial position. It was confirmed that the maximum coolant temperature occurred in the recirculation region downstream from the blockage, which is about 580 ℃. This is more than the temperature calculated at the end of the active region.

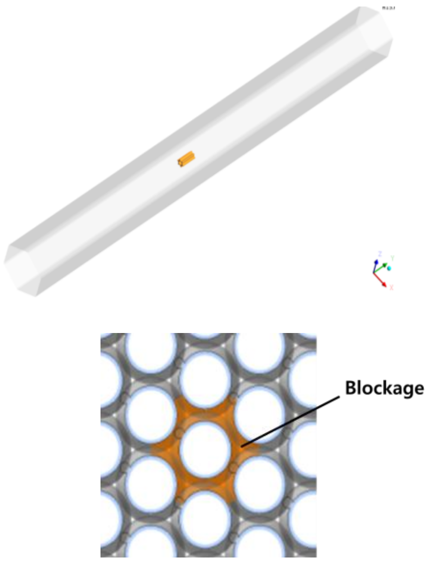

Figure 10. Computational domain for the CFD: blockage position

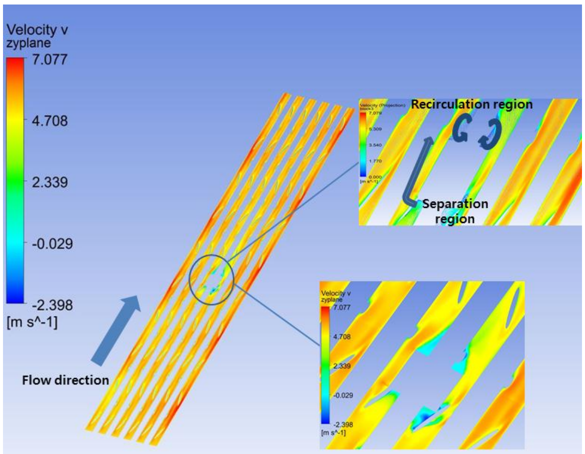

Figure 11 Streamwise velocity contours in the ZX midplane.

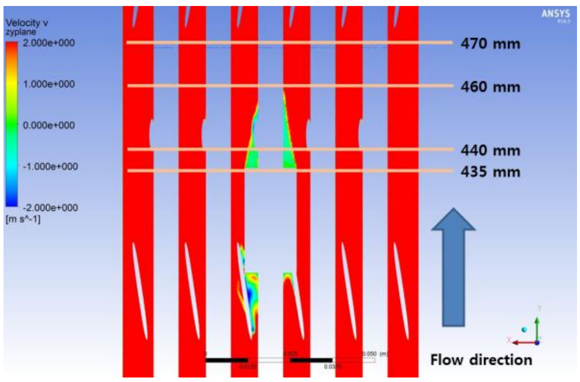

Figure 12 velocity contours downstream the blockage

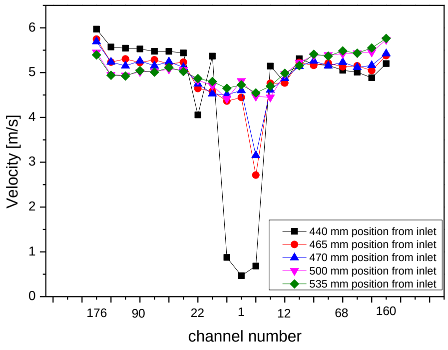

Figure 13 Velocity distributions in the symmetry ZX planes from the start of inlet

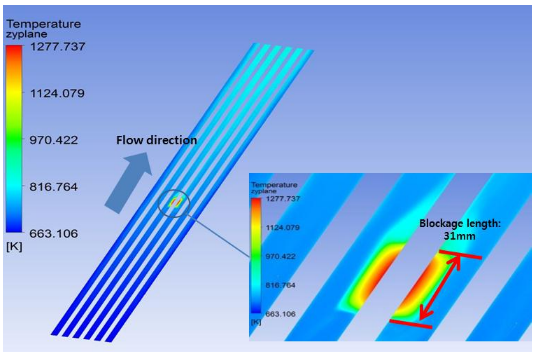

Figure 14 Temperature contours in the ZX.

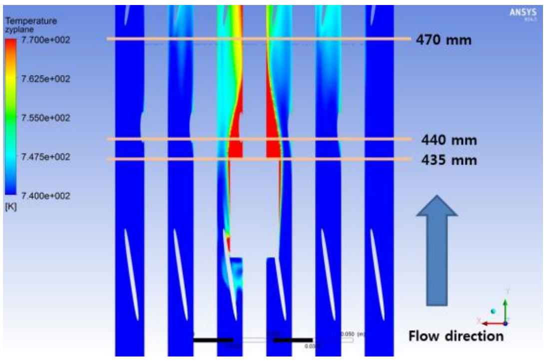

Figure 15 Temperature contours downstream the blockage

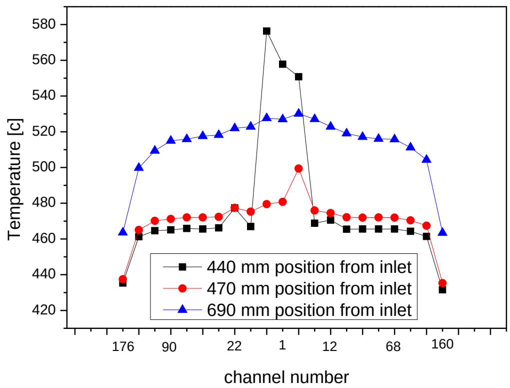

Figure 16 Temperature distributions in the symmetry ZX planes from the start of inlet

4. Conclusions

A CFD analysis using fully resolved RANS simulations has been carried out on the fluid flow and heat transfer in the case of a flow blockage for fuel assemblies in a PGSFR. A fuel assembly with 91 pins instead of all 217 pins was considered for this study. Two main effects can be distinguished in a flow blockage: a locally lower mass flow rate in the wake/recirculation region downstream of the blockage, and the peak temperature behind the blockage. Both of them are closely related. The recirculation region exists within a short distance downstream from the blockage, and it has an effect on the cladding integrity. The maximum cladding temperature is about 1000 ℃ and is located in the central pins of the blockage region. It could lead to a rupture of the cladding. From these analysis results, the axial blockage size may have a significant impact on the clad integrity.

REFERENCES

[1] W. P. Chang et al., “The Analysis of Partial Flow Blockage Accidents for a Sodium Cooled Fast Reactor,” Proceedings of ICONE20, July 30-August 3, 2012, Anaheim, California, USA (2012)

[2] Y. M. Kwon et al., “Technical consultation report on flow blockage analysis methodologies,” Work order KA-SA-99-01, KAERI, Korea, Dec. 10 (1999)

[3] Fontana, M. H. et al., 1973. “Effect of partial blockages in simulated LMFBR fuel assemblies,” ORNL-TM-4324, Oak Ridge National Laboratory.

[4] Mansour, Talebi. et al., “Investigation of effects of helical wire-wrapped spacers on thermo hydraulic properties of a fluid flow along to heated fuel bundle,” International Journal of Application or Innovation in Engineering & Management, Nov, 2013